Communications in Theoretical Physics

PAPER

Significance of Darcy-Forchheimer Porous Medium in Nanofluid Through Carbon Nanotubes

To cite this article: Taseer Muhammad *et al* 2018 *Commun. Theor. Phys.* **70** 361

Significance of Darcy-Forchheimer Porous Medium in Nanofluid Through Carbon Nanotubes

Taseer Muhammad,[1,2,*] Dian-Chen Lu,[1,†] B. Mahanthesh,[3] Mohamed R. Eid,[4,8] Muhammad Ramzan,[5,6] and Amanullah Dar[7]

[1]Department of Mathematics, Faculty of Science, Jiangsu University, Zhenjiang 212013, China

[2]Department of Mathematics, Government College Women University, Sialkot 51310, Pakistan

[3]Department of Mathematics, Christ University, Bengaluru 560029, Karnataka, India

[4]Department of Mathematics, Faculty of Science, New Valley Branch, Assiut University, Assiut 71511, Egypt

[5]Department of Computer Science, Bahria University, Islamabad Campus, Islamabad 44000, Pakistan

[6]Department of Mechanical Engineering, Sejong University, Seoul 143-747, South Korea

[7]Department of Mathematics, University of Kotli Azad Jammu and Kashmir, Kotli 11100, Pakistan

[8]Department of Basic Science, Deanship of Preparatory Year, Northern Border University, Arar 91431, Saudi Arabia

(Received April 8, 2018)

Abstract *This article manages Darcy-Forchheimer 3D flow of water based carbon nanomaterial (CNTs). A bidirectional nonlinear stretchable surface has been utilized to make the flow. Disturbance in permeable space has been represented by Darcy Forchheimer (DF) expression. Heat transfer mechanism is explored through convective heating. Outcomes for SWCNT and MWCNT have been displayed and compared. The reduction of partial differential framework into nonlinear common differential framework is made through reasonable variables. Optimal series scheme is utilized for arrangements advancement of associated flow issue. Optimal homotopic solution expressions for velocities and temperature are studied through graphs by considering various estimations of physical variables. Moreover surface drag coefficients and heat transfer rate are analyzed through plots.*

DOI: 10.1088/0253-6102/70/3/361

Key words: three-dimensional flow, CNTs (SWCNT and MWCNT), Darcy-Forchheimer porous space, convective surface condition, nonlinear stretching surface

Nomenclature

u, v, w	velocity components	n	power-law index
x, y, z	space coordinates	U_w, V_w	surface stretching velocities
μ_f	fluid dynamic viscosity	ρ_f	fluid density
ν_f	kinematic fluid viscosity	$\nu_{\rm nf}$	kinematic nanofluid viscosity
k_f	basefluid themal conductivity	$k_{\rm nf}$	nanofluids themal conductivity
α_f	thermal diffusivity of base fluid	$\alpha_{\rm nf}$	thermal diffusivity of nanofluid
T_f	hot fluid temperature	T_∞	ambient fluid temperature
h_f	heat transfer coefficient	$k_{\rm CNT}$	CNTs thermal conductivity
a, b	positive constants	k^*	permeability of porous medium
F	non-uniform inertia coefficient	ϕ	nanomaterial volume fraction
C_b	drag coefficient	Re_x, Re_y	local Reynolds numbers
C_f, C_g	skin friction coefficients	Nu	local Nusselt number
λ	local porosity number	η	dimensionless variable
Fr	Forchheimer parameter	f', g'	dimensionless velocities
Bi	Biot parameter	θ	dimensionless temperature
Pr	Prandtl parameter	α	ratio number
CNTs	carbon nanotubes	Z_j^{**}	arbitrary constants

*Corresponding author, E-mail: taseer_qau@yahoo.com

†Corresponding author, E-mail: dclu@ujs.edu.cn

1 Introduction

Carbon nanotubes are the least difficult compound sythesis and nuclear holding arrangement of graphene sheet structures moved up in a state of chamber. Carbon nanotubes have special physical, electrical, thermal, chemical, and mechanical properties, because of the blend of their little size, tube shaped structure and colossal surface region. Contingent upon the quantity of graphene layers, carbon nanotubes have been subdivided in two sorts that is single walled carbon nanotubes (SWCNT) and multi walled carbon nanotubes (MWCNT). Anomalous heat conductivity improvement in oil-based nanofluids containing carbon nanotube is represented by Choi *et al.*[1] Xue[2] proposed a model in view of Maxwell hypothesis for transport properties of CNTs based composites. Aueous suspensions of multi-walled carbon nanotubes is investigated by Ding *et al.*[3] Few commitments toward this path can be looked into through the attempts[4−25] and different examinations therein.

Flow of liquid through permeable space assumes essential part in different mechanical applications, for example, warm protection designing, water developments in geothermal supplies, underground spreading of substance squander, atomic waste archive, grain stockpiling, upgraded recuperation of oil stores, improved oil recuperation, land carbon-dioxide sequestration, pressed cryogenic microsphere protection, coordinate contact warm exchangers, coal combustors, atomic waste storehouses, and warmth pipe innovation. For flow under low velocity and weak porosity conditions, Darcy developed a pioneering semi-empirical equation. Nonlinearity appears in semi-empirical equation for high Reynolds number which is due to increasing role of inertial forces. Forchheimer[26] predicted a modified equation namely Darcy-Forchheimer equation by introducing quadratic term in momentum equation. Muskat[27] entitled it as Forchheimer factor. Having above in view, further relevant studies on Darcy-Forchheimer flow can be looked into through the attempts[28−38] and different examinations therein.

The prime point of this endeavor is to investigate Darcy Forchheimer (DF) three-dimensional (3D) flow of carbon water nanomaterials. Flow created is a result of nonlinear stretchable surface. Heat exchange component is investigated by means of convective surface condition. Single walled (SWCNT) and multi walled (MWCNT) carbon nanotubes are considered. Xue model is implemented in mathematical modeling. The governing nonlinear system is solved by optimal homotopic approach.[39−45] Effectiveness of sundry factors on temperature and velocities fields are analyzed. Additionally skin frictions and Nusselt number are introduced by means of plots.

2 Formulation

We consider three dimension (3D) flow of water based carbon nanomaterials (CNTs) caused by nonlinear stretchable surface in a Darcy-Forchheimer permeable space. Temperature at surface is controlled via convection, which is described by hot fluid at temperature T_f below the surface and heat transfer coefficient h_f. The surface at $z = 0$ possessing the stretching velocities $U_w(x, y) = a(x+y)^n$ and $V_w(x, y) = b(x+y)^n$ where a, b, and $n > 0$ are the positive constants (see Fig. 1). SWCNT and MWCNT are utilized as nanomaterials in water. The problems statements are:[10,31]

$$\frac{\partial u}{\partial x}+\frac{\partial v}{\partial y}+\frac{\partial w}{\partial z}=0\,, \tag{1}$$

$$u\frac{\partial u}{\partial x}+v\frac{\partial u}{\partial y}+w\frac{\partial u}{\partial z}=v_{\rm nf}\frac{\partial^2 u}{\partial z^2}-\frac{v_{\rm nf}}{k^*}u-Fu^2, \tag{2}$$

$$u\frac{\partial v}{\partial x}+v\frac{\partial v}{\partial y}+w\frac{\partial v}{\partial z}=v_{\rm nf}\frac{\partial^2 v}{\partial z^2}-\frac{v_{\rm nf}}{k^*}v-Fv^2, \tag{3}$$

$$u\frac{\partial T}{\partial x}+v\frac{\partial T}{\partial y}+w\frac{\partial T}{\partial z}=\alpha_{\rm nf}\frac{\partial^2 T}{\partial z^2}\,. \tag{4}$$

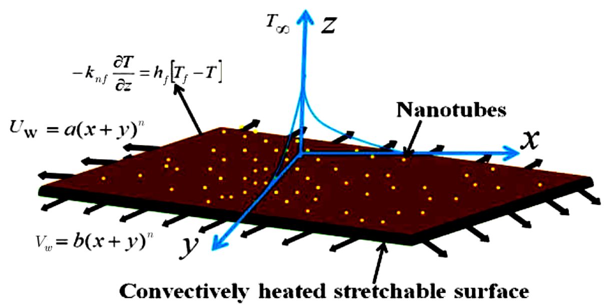

Fig. 1 Physical configuration and coordinate system.

The associated boundary conditions are:[10,31]

$$u=U_w,\quad v=V_w,\quad w=0$$
$$-k_{\rm nf}\Big(\frac{\partial T}{\partial z}\Big)=h_f(T_f-T)\ \text{at}\ z=0\,, \tag{5}$$

$$u\to 0,\quad v\to 0,\quad T\to T_\infty\ \text{as}\ z\to\infty\,. \tag{6}$$

Here u, v, and w stand for fluid velocities in x-, y-, and z-axes, C_b for drag coefficient, $\nu_{\rm nf}$ for kinematic viscosity of nanofluid, $F = C_b/[(x+y)k^{*\frac{1}{2}}]$ for nonuniform inertia coefficient of permeable space, k^* for permeability of permeable space, $\alpha_{\rm nf}$ for nanofluid thermal diffusivity, T for temperature, T_f for hot fluid temperature, and T_∞ for ambient temperature and c_p for specific heat. Theoretical relation suggested by Xue[2] is defined as follows:

$$v_{\rm nf}=\frac{\mu_{\rm nf}}{\rho_{\rm nf}},\quad \mu_{\rm nf}=\frac{\mu_f}{(1-\phi)^{2.5}}\,,$$
$$\frac{k_{\rm nf}}{k_f}=\frac{(1-\phi)+2\phi\frac{k_{\rm CNT}}{k_{\rm CNT}-k_f}\ln\frac{k_{\rm CNT}+k_f}{2k_f}}{(1-\phi)+2\phi\frac{k_f}{k_{\rm CNT}-k_f}\ln\frac{k_{\rm CNT}+k_f}{2k_f}}\,,$$
$$\rho_{\rm nf}=(1-\phi)\rho_f+\phi\rho_{\rm CNT},\quad \alpha_{\rm nf}=\frac{k_{\rm nf}}{\rho_{\rm nf}(c_p)_{\rm nf}}\,, \tag{7}$$

in which $\mu_{\rm nf}$ stands for nanofluid viscosity, ϕ for nanoparticle fraction, $\rho_{\rm nf}$ for nanofluid density, $k_{\rm nf}$ for nanofluid heat conductivity, $\rho_{\rm CNT}$ for CNTs density and $k_{\rm CNT}$ for carbon nanotubes thermal conductivity. Table 1 exhibits physical attributes of water and CNTs.

Table 1 Physical aspects of water and CNTs.[2]

Physical aspects	Base fluid	CNTs	
	Water	SWCNTs	MWCNTs
ρ	997.1	2600	1600
c_p	4179	425	796
k	0.613	6600	3000

Using the appropriate transformations:

$$u = a(x+y)^n f'(\eta), \quad v = a(x+y)^n g'(\eta),$$
$$w = -\Big(\frac{a\nu_f(n+1)}{2}\Big)^{1/2}(x+y)^{(n-1)/2} \times \Big((f+g) + \frac{n-1}{n+1}\eta(f'+g')\Big),$$
$$\theta(\eta) = \frac{T-T_\infty}{T_f - T_\infty},$$
$$\eta = \Big(\frac{a(n+1)}{2v_f}\Big)^{1/2}(x+y)^{(n-1)/2} z. \tag{8}$$

Now Eq. (1) is verified while Eqs. (2)–(7) have been reduced to

$$\frac{1}{(1-\phi)^{2.5}[1-\phi+\phi(\rho_{\rm CNT}/\rho_f)]} f''' + (f+g)f'' - \frac{2n}{(n+1)}(f'+g')f' - \frac{2}{(n+1)}\frac{\lambda}{(1-\phi)^{2.5}[1-\phi+\phi(\rho_{\rm CNT}/\rho_f)]} f' - \frac{2}{n+1} Fr (f')^2 = 0, \tag{9}$$

$$\frac{1}{(1-\phi)^{2.5}[1-\phi+\phi(\rho_{\rm CNT}/\rho_f)]} g''' + (f+g)g'' - \frac{2n}{(n+1)}(f'+g')g' - \frac{2}{(n+1)}\frac{\lambda}{(1-\phi)^{2.5}[1-\phi+\phi(\rho_{\rm CNT}/\rho_f)]} g' - \frac{2}{n+1} Fr (g')^2 = 0, \tag{10}$$

$$\frac{1}{[1+\phi+\phi((\rho c_p)_{\rm CNT}/(\rho c_{P})_f)]}\frac{k_{\rm nf}}{k_f}\theta'' + Pr(f+g)\theta' = 0, \tag{11}$$

$$f(0) = g(0) = 0, \quad f'(0) = 1, \quad g'(0) = \alpha, \quad \theta'(0) = -\sqrt{\frac{n+1}{2}}\frac{k_{\rm nf}}{k_f} Bi(1-\theta(0)), \tag{12}$$

$$f'(\infty) \to 0, \quad g'(\infty) \to 0, \quad \theta(\infty) \to 0. \tag{13}$$

Here Fr stands for Forchheimer parameter, α for ratio number, λ for local porosity number, Bi for Biot parameter and Pr for Prandtl parameter. These variables are defined by

$$\lambda = \frac{v_f}{k^* a(x+y)^{n-1}}, \quad Fr = \frac{C_b}{k^{*\frac{1}{2}}}, \quad Pr = \frac{\mu_f (c_p)_f}{k_f},$$
$$\alpha = \frac{b}{a}, \quad Bi = \frac{h_f}{k_f}\sqrt{\frac{(x+y)^{n-1}}{a}}. \tag{14}$$

Skin frictions and Nusselt number are expressed by

$$C_f Re_x^{1/2} = \sqrt{\frac{n+1}{2}}\frac{1}{(1-\phi)^{2.5}} f''(0), \tag{15}$$

$$C_g Re_y^{1/2} = \alpha^{-3/2}\sqrt{\frac{n+1}{2}}\frac{1}{(1-\phi)^{2.5}} g''(0), \tag{16}$$

$$Nu\, Re_x^{-1/2} = -\sqrt{\frac{n+1}{2}}\frac{k_{\rm nf}}{k_f}\theta'(0), \tag{17}$$

where $Re_x = U_w(x+y)/\nu_f$ and $Re_y = V_w(x+y)/\nu_f$ stand for local Reynolds numbers.

3 OHAM Solutions

The optimal series arrangements of Eqs. (9) to (11) via (12) and (13) are developed by employing optimal homotopic technique (OHAM). Operators and initial deformations are chosen as follows:

$$f_0(\eta) = 1 - \exp(-\eta), \quad g_0(\eta) = \alpha(1-\exp(-\eta)),$$
$$\theta_0(\eta) = \frac{B_i}{(\sqrt{(n+1)/2}(k_{\rm nf}/k_f) + B_i)}\exp(-\eta), \tag{18}$$

$$\pounds_f(f) = \frac{{\rm d}^3 f}{{\rm d}\eta^3} - \frac{{\rm d}f}{{\rm d}\eta}, \quad \pounds_g(g) = \frac{{\rm d}^3 g}{{\rm d}\eta^3} - \frac{{\rm d}g}{{\rm d}\eta},$$
$$\pounds_\theta(\theta) = \frac{{\rm d}^2\theta}{{\rm d}\eta^2} - \theta. \tag{19}$$

The above linear operators obey

$$\pounds_f[Z_1^{**} + Z_2^{**}\exp(\eta) + Z_3^{**}\exp(-\eta)] = 0,$$
$$\pounds_g[Z_4^{**}\exp(\eta) + Z_5^{**}\exp(-\eta)] = 0,$$
$$\pounds_\theta[Z_6^{**}\exp(\eta) + Z_7^{**}\exp(-\eta)] = 0, \tag{20}$$

where Z_j^{**} ($j = 1$–7) stand for arbitrary variables. Problems for m-th order and zeroth deformations are easily constructed in the view of above operators. The associated deformation issues are solved via BVPh2.0 of *Mathematica* package.

4 Convergence Analysis

We have solved the momentum and energy expressions with the help of BVPh2.0. These expressions contain unknown variables $\hbar_f$, $\hbar_g$, and $\hbar_\theta$. We can compute the minimum estimation of these variables by taking total error small. In the edge of HAM, these factors assume a fundamental part. That is the reason these factors allude to as convergence control factor which varies HAM from other scientific guess strategies. Keeping in mind the end goal to diminish CPU time, we have utilized average residual errors at m-th oder of guess, which are characterized by

$$\varepsilon_m^f = \frac{1}{k+1}\sum_{j=0}^{k}\Big[\mathcal{N}_f\Big(\sum_{i=0}^{m}\hat{f}(\eta),\ \sum_{i=0}^{m}\hat{g}(\eta)\Big)_{\eta=j\delta\eta}\Big]^2, \tag{21}$$

$$\varepsilon_m^g = \frac{1}{k+1}\sum_{j=0}^{k}\Big[\mathcal{N}_g\Big(\sum_{i=0}^{m}\hat{f}(\eta),\ \sum_{i=0}^{m}\hat{g}(\eta)\Big)_{\eta=j\delta\eta}\Big]^2, \tag{22}$$

$$\varepsilon_m^\theta = \frac{1}{k+1}\sum_{j=0}^{k}\Big[\mathcal{N}_\theta\Big(\sum_{i=0}^{m}\hat{f}(\eta),\sum_{i=0}^{m}\hat{g}(\eta),\ \sum_{i=0}^{m}\hat{\theta}(\eta)\Big)_{\eta=j\delta\eta}\Big]^2. \tag{23}$$

Following Liao:[39]

$$\varepsilon_m^t = \varepsilon_m^f + \varepsilon_m^g + \varepsilon_m^\theta\,, \tag{24}$$

where ε^t represents the total residual squared error, $k = 20$ and $\delta\eta = 0.5$. Optimal information of convergence control factors at 2nd order of distortions is $h_f = -0.8118$, $h_g = -0.9927$, and $h_\theta = -1.563\ 92$ for SWCNT-Water and $h_f = -0.8428$, $h_g = -1.062\ 73$ and $h_\theta = -1.560\ 89$ for MWCNT-Water. Table 2 displays average square residual error at various request of distortions. It has been broke down that the average residual square errors reduce with higher request distortions for SWCNT and MWCNT.

Table 2 Individual average residual square errors employing optimal estimations of auxiliary factors.

	SWCNT			MWCNT		
m	ε_m^f	ε_m^g	ε_m^θ	ε_m^f	ε_m^g	ε_m^θ
2	6.16×10^{-6}	1.46×10^{-6}	1.13×10^{-3}	1.03×10^{-5}	1.99×10^{-6}	1.23×10^{-3}
6	1.03×10^{-9}	1.59×10^{-10}	1.18×10^{-4}	4.70×10^{-9}	4.95×10^{-10}	1.56×10^{-4}
8	2.06×10^{-11}	3.39×10^{-12}	5.67×10^{-5}	1.69×10^{-10}	1.68×10^{-11}	8.22×10^{-5}
10	4.56×10^{-13}	9.95×10^{-14}	3.06×10^{-5}	7.26×10^{-12}	7.03×10^{-13}	4.86×10^{-5}
14	2.39×10^{-16}	1.35×10^{-16}	1.11×10^{-5}	1.80×10^{-14}	1.70×10^{-15}	2.11×10^{-5}
18	7.36×10^{-19}	2.72×10^{-19}	4.85×10^{-6}	5.76×10^{-17}	5.34×10^{-18}	1.09×10^{-5}
20	1.91×10^{-20}	1.34×10^{-20}	3.35×10^{-6}	3.45×10^{-18}	3.17×10^{-19}	8.23×10^{-6}

5 Discussion

The present segment inspects impacts of various physical elements like nanoparticles fraction parameter ϕ, local porosity number λ, Forchheimer parameter Fr, ratio number α, and Biot parameter Bi on velocities $f'(\eta)$ and $g'(\eta)$ and temperature $\theta(\eta)$. Outcomes are achieved for single walled CNTs and mutli walled CNTs. Figure 2 signifies the effect of volume division of nanoparticles ϕ on velocity field $f'(\eta)$. It is accounted for that velocity field $f'(\eta)$ upgrades for bigger ϕ for SWCNT and MWCNT. The role of local porosity number λ on velocity field $f'(\eta)$ is portrayed in Fig. 3. It is investigated that velocity $f'(\eta)$ decays for higher λ for SWCNT and MWCNT. Physically the obstruction is created in liquid flow because of presence of permeable space, which portrays a diminishment in liquid velocity. Hence a lessening is noted in the velocity and momentum layer. From Fig. 4, it is revealed that velocity field $f'(\eta)$ begins diminishing with an expansion in Forchheimer parameter Fr for SWCNT and MWCNT. Figure 5 displays the impact of solid volume fraction of nanoparticles ϕ on velocity field $g'(\eta)$. It is reported that velocity field $g'(\eta)$ is enhanced for larger ϕ for SWCNT and MWCNT. The behavior of local porosity number λ on velocity field $g'(\eta)$ is plotted in Fig. 6.

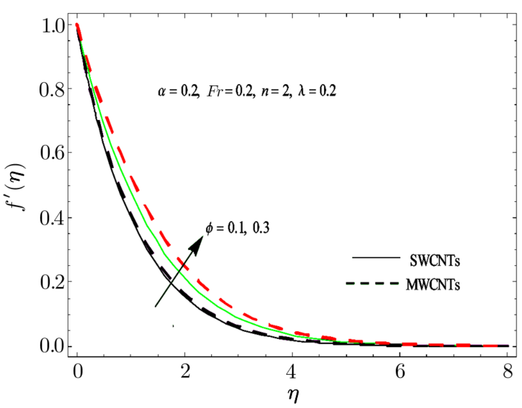

Fig. 2 Effect of ϕ on $f'(\eta)$.

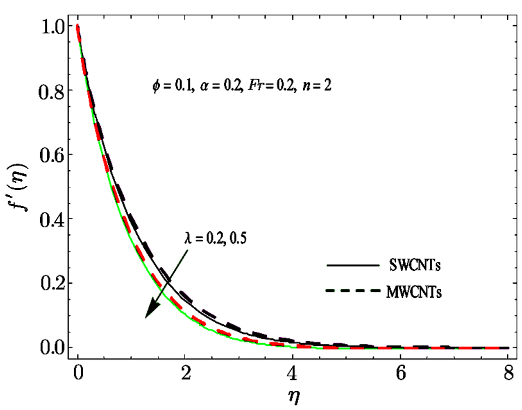

Fig. 3 Effect of λ on $f'(\eta)$.

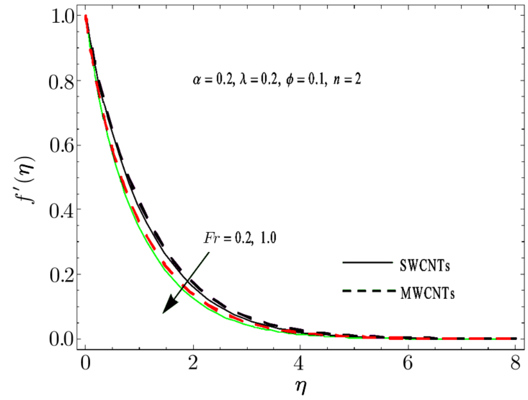

Fig. 4 Effect of Fr on $f'(\eta)$.

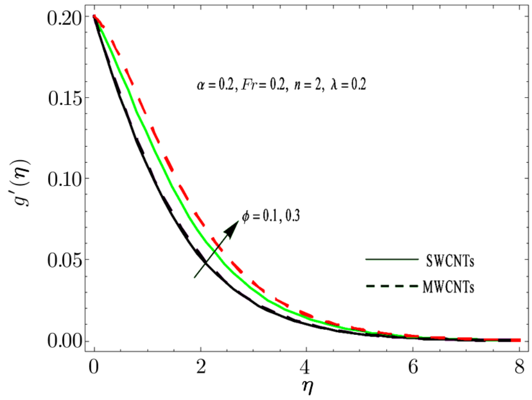

Fig. 5 Effect of ϕ on $g'(\eta)$.

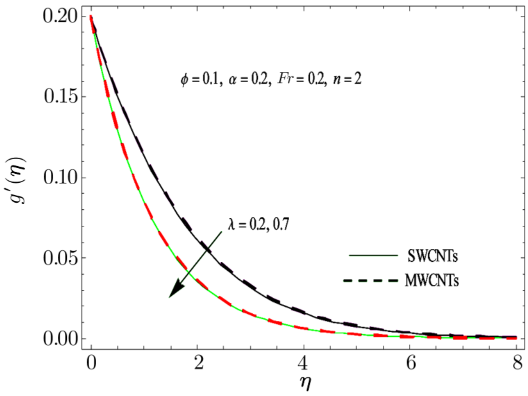

Fig. 6 Effect of λ on $g'(\eta)$.

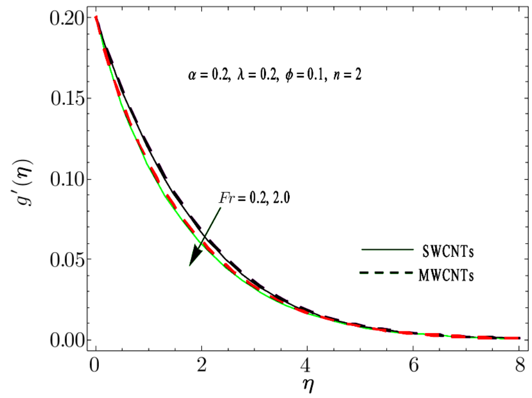

Fig. 7 Effect of Fr on $g'(\eta)$.

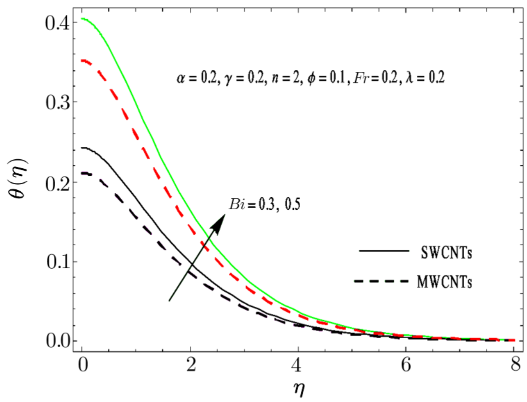

Fig. 8 Effect of Bi on $\theta(\eta)$.

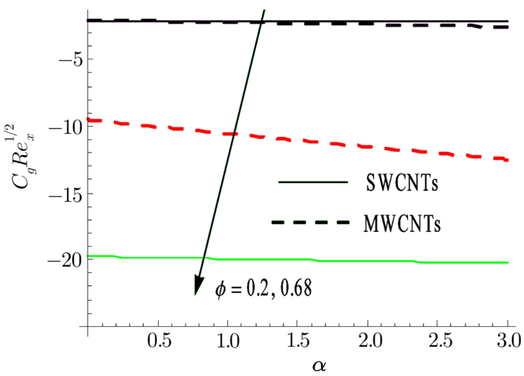

Fig. 9 Effects of α and ϕ on $C_f Re_x^{1/2}$.

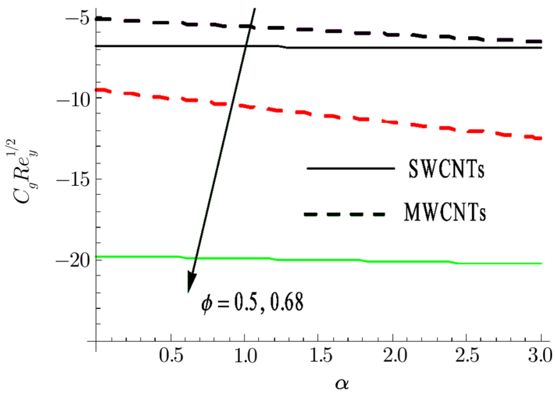

Fig. 10 Effects of α and ϕ on $C_g Re_y^{1/2}$.

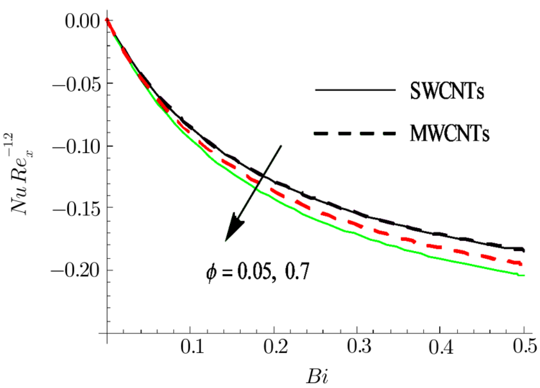

Fig. 11 Effects of Bi and ϕ on $Nu\, Re_x^{-1/2}$.

It is watched that velocity field $g'(\eta)$ reduces for higher λ for SWCNT and MWCNT. From Fig. 7, it is noted that velocity field $g'(\eta)$ diminishes with an expansion in Forchheimer parameter Fr for SWCNT and MWCNT. Effect of Biot parameter Bi on temperature field $\theta(\eta)$ is plotted in Fig. 8. Here temperature field $\theta(\eta)$ upgrades for higher Biot parameter Bi for SWCNT and MWCNT. Bigger Biot parameter causes a more grounded convection which yields a more grounded temperature $\theta(\eta)$ and more thermal layer. Figures 9 and 10 present skin frictions $C_f Re_x^{1/2}$ and $C_g Re_y^{1/2}$ for several estimations of nanoparticles fraction ϕ and ratio number α. It is watched that skin frictions are improved for expanding estimations of nanoparticles fraction parameter for SWCNT and MWCNT. From Fig. 11, it is analyzed that Nusselt number $Nu\, Re_x^{-1/2}$ improves for bigger nanoparticles fraction parameter ϕ for SWCNT and MWCNT.

6 Conclusions

Darcy Forchheimer 3D flow of carbon water nanomaterials (CNTs) within the sight of thermal convective condition is considered. Flow is caused by a bi-directional nonlinear stretchable surface. Optimal homotopic calculation prompts the arrangements of representing flow issue. We have seen that velocities indicate comparative pattern for local porosity number and Forchheimer parameter. An enhancement in Biot parameter exhibits stronger temperature field. Moreover skin frictions and local Nusselt number show increasing trend for higher nanoparticle fraction parameter.

References

[1] S. U. S. Choi, Z. G. Zhang, W. Yu, *et al.*, Appl. Phys. Lett. **79** (2001) 2252.
[2] Q. Z. Xue, Physica B: Condensed Matter **368** (2005) 302.
[3] Y. Ding, H. Alias, D. Wen, and R. A. Williams, Int. J. Heat Mass Transfer **49** (2006) 240.
[4] J. Wang, J. Zhu, X. Zhang, and Y. Chen, Exp. Therm. Fluid Sci. **44** (2013) 716.
[5] M. R. Safaei, H. Togun, K. Vafai, *et al.*, Numerical Heat Transfer, Part A **66** (2014) 1321.
[6] R. Ellahi, M. Hassan, and A. Zeeshan, IEEE Trans. Nanotech. **14** (2015) 726.
[7] T. Hayat, Z. Hussain, T. Muhammad, and A. Alsaedi, J. Mol. Liq. **221** (2016) 1121.
[8] Z. Iqbal, E. Azhar, and E. N. Maraj, Physica E: Low-dimensional Systems and Nanostructures **91** (2017) 128.
[9] U. Khan, N. Ahmed, and S. T. Mohyud-Din, Appl. Thermal Eng. **113** (2017) 1107.
[10] T. Hayat, S. Ahmed, T. Muhammad, *et al.*, Results Phys. **7** (2017) 2651.
[11] T. Hayat, F. Haider, T. Muhammad, and A. Alsaedi, Int. J. Heat Mass Transfer **112** (2017) 248.
[12] R. Ellahi, M. H. Tariq, M. Hassan, and K. Vafai, J. Mol. Liq. **229** (2017) 339.
[13] S. Rashidi, J. A. Esfahani, and R. Ellahi, Appl. Sci. **7** (2017) 431.
[14] T. Hayat, R. Sajjad, T. Muhammad, *et al.*, Results Phys. **7** (2017) 535.
[15] J. A. Esfahani, M. Akbarzadeh, S. Rashidi, *et al.*, Int. J. Heat Mass Transfer **109** (2017) 1162.
[16] M. Hassan, A. Zeeshan, A. Majeed, and R. Ellahi, J. Magn. Magn. Mater. **443** (2017) 36.
[17] T. Hayat, R. Sajjad, A. Alsaedi, *et al.*, Results Phys. **7** (2017) 553.
[18] R. Ellahi, Appl. Sci. **8** (2018) 192.
[19] A. Zeeshan, N. Shehzad, and R. Ellahi, Results Phys. **8** (2018) 502.
[20] N. Ijaz, A. Zeeshan, M. M. Bhatti, and R. Ellahi, J. Mol. Liq. **250** (2018) 80.
[21] S. Rashidi, S. Akar, M. Bovand, and R. Ellahi, Renewable Energy **115** (2018) 400.
[22] M. R. Eid, K. L. Mahny, T. Muhammad, and M. Sheikholeslami, Results Phys. **8** (2018) 1185.
[23] M. Sheikholeslami, T. Hayat, T. Muhammad, and A. Alsaedi, Int. J. Mech. Sci. **135** (2018) 532.
[24] T. Hayat, K. Muhammad, T. Muhammad, and A. Alsaedi, Commun. Theor. Phys. **69** (2018) 441.
[25] T. Hayat, F. Haider, T. Muhammad, and A. Alsaedi, J. Phys. Chem. Solids **120** (2018) 79.
[26] P. Forchheimer, Zeitschrift Ver. D Ing. **45** (1901) 1782.
[27] M. Muskat, *The Flow of Homogeneous Fluids Through Porous Media*, Edwards, MI (1946).
[28] M. A. Seddeek, J. Colloid Interface Sci. **293** (2006) 137.
[29] T. Hayat, T. Muhammad, S. Al-Mezal, and S. J. Liao, Int. J. Numer. Methods Heat Fluid Flow **26** (2016) 2355.
[30] S. A. Bakar, N. M. Arifin, R. Nazar, *et al.*, Frontiers Heat Mass Transfer **7** (2016) 38.
[31] T. Hayat, A. Aziz, T. Muhammad, and A. Alsaedi, Commun. Theor. Phys. **68** (2017) 387.
[32] J. C. Umavathi, O. Ojjela, and K. Vajravelu, Int. J. Thermal Sci. **111** (2017) 511.
[33] T. Hayat, F. Haider, T. Muhammad, and A. Alsaedi, Results Phys. **7** (2017) 2663.
[34] T. Muhammad, A. Alsaedi, S. A. Shehzad, and T. Hayat, Chin. J. Phys. **55** (2017) 963.
[35] T. Hayat, F. Haider, T. Muhammad, and A. Alsaedi, J. Mol. Liq. **233** (2017) 278.
[36] T. Muhammad, A. Alsaedi, T. Hayat, and S. A. Shehzad, Results Phys. **7** (2017) 2791.
[37] T. Hayat, K. Rafique, T. Muhammad, *et al.*, Results Phys. **8** (2018) 26.
[38] T. Hayat, F. Haider, T. Muhammad, and A. Alsaedi, Results Phys. **8** (2018) 764.
[39] S. J. Liao, Commun. Nonlinear. Sci. Numer. Simul. **15** (2010) 2003.
[40] A. Malvandi, F. Hedayati, and G. Domairry, J. Thermodynamics **2013** (2013) 764827.
[41] T. Hayat, T. Muhammad, A. Alsaedi, and M. S. Alhuthali, J. Magn. Magn. Mater. **385** (2015) 222.
[42] M. Turkyilmazoglu, Filomat **30** (2016) 1633.
[43] A. Zeeshan, A. Majeed, and R. Ellahi, J. Mol. Liq. **215** (2016) 549.
[44] T. Hayat, S. Ahmed, T. Muhammad, and A. Alsaedi, Physica E: Low-dimensional Systems and Nanostructures **94** (2017) 70.
[45] T. Muhammad, T. Hayat, S. A. Shehzad, and A. Alsaedi, Results Phys. **8** (2018) 365.